

Generation of a Novel A Kinase Anchor Protein and a Myristoylated Alanine-rich C Kinase Substrate-like Analog from a Single Gene*

(Received for publication, March 10, 1999, and in revised form, July 1, 1999)

Zhuo Li[‡], Edmund A. Rossi[‡], Jörg D. Hoheisel[§], Daniel Kalderon[¶], and Charles S. Rubin[‡]||

From the [‡]Department of Molecular Pharmacology, Atran Laboratories, Albert Einstein College of Medicine, Bronx, New York 10461, the [§]Department of Molecular Genetic Genome Analysis, Deutsches Krebsforschungszentrum, Im Neuenheimer Feld 506, D-69120 Heidelberg, Germany, and the [¶]Department of Biological Sciences, Columbia University, New York, New York 10027

A unique *Drosophila* gene encodes two novel signaling proteins. *Drosophila* A kinase anchor protein 200 (DAKAP200) (753 amino acids) binds regulatory subunits of protein kinase AII (PKAII) isoforms *in vitro* and in intact cells. The acidic DAKAP200 polypeptide (pI ~3.8) contains an optimal N-terminal myristoylation site and a positively charged domain that resembles the multifunctional phosphorylation site domain of vertebrate myristoylated alanine-rich C kinase substrate proteins. The 15-kilobase pair DAKAP200 gene contains six exons and encodes a second protein, Δ DAKAP200. Δ DAKAP200 is derived from DAKAP200 transcripts by excision of exon 5 (381 codons), which encodes the PKAII binding region and a Pro-rich sequence. Δ DAKAP200 appears to be a myristoylated alanine-rich C kinase substrate analog. DAKAP200 and Δ DAKAP200 are evident *in vivo* at all stages of *Drosophila* development. Thus, both proteins may play important physiological roles throughout the life span of the organism. Nevertheless, DAKAP200 gene expression is regulated. Maximal levels of DAKAP200 are detected in the pupal phase of development; Δ DAKAP200 content is elevated 7-fold in adult head (brain) relative to other body parts. Enhancement or suppression of exon 5 excision during DAKAP200 pre-mRNA processing provides potential mechanisms for regulating anchoring of PKAII and targeting of cAMP signals to effector sites in cytoskeleton and/or organelles.

Cyclic AMP-dependent protein kinases (PKAs)¹ mediate actions of hormones that stimulate adenylate cyclase (1–4). Signals carried by cAMP often regulate activities of proteins that accumulate at discrete intracellular locations (e.g. ion channels in plasma membrane) (5–8). A kinase anchor proteins (AKAPs) guide transmission and routing of cAMP signals to such micro-

environments. AKAPs have an avid binding site for regulatory subunits (RII) of PKAII isoforms² and distinct domains that target the tethered PKA holoenzyme to docking sites in organelles or cytoskeleton (5, 6, 9, 10). Accumulation of a high concentration of anchored PKAII in proximity with clustered substrate-effector protein promotes efficient reception, amplification, and precisely focused transmission of signals borne by cAMP (5–8).

Several fundamental questions about AKAP-RII complexes remain unresolved. Current models suggest that AKAPs statically associate with docking sites in organelles. However, it is possible that AKAP-RII complexes shuttle dynamically between intracellular loci. This proposition has neither been excluded nor systematically investigated. Many physiological processes are coordinately regulated by groups of hormones. Homeostatic control is often achieved through synergistic or antagonistic interactions among signaling pathways that are activated by different second messenger molecules. A key question is how signals transmitted via AKAP-PKAII complexes are integrated with inputs from pathways controlled by other second messengers in order to regulate common effector proteins. PKA anchoring may be regulated by pretranslational mechanisms. In thyroid-derived cells, activation of adenylate cyclase elicits AKAP121 gene transcription and accumulation of AKAP121 mRNA and protein (11). However, hormonal activation of transcription of other AKAP genes has not been demonstrated. Could the concentration of anchored PKAII be governed by a post-transcriptional mechanism?

Drosophila melanogaster provides an attractive model system for addressing questions posed above. Signaling pathways, molecules, and mechanisms used in *Drosophila* are conserved in mammals (12). Classical and molecular genetics indicate that accumulation and activation of PKA at discrete intracellular locations are essential for normal development and reproduction in *Drosophila* (13–15). Consequences of localized activation of PKA are proper anterior-posterior patterning in developing tissues, maintenance of intercellular bridges between nurse cells and oocytes, and remodeling of the microtubule-based cytoskeleton that changes microtubule polarity in embryos and facilitates differential segregation of mRNAs (14–18). *Drosophila* express PKAI-, PKAII-, and high affinity RII-binding proteins (13, 19, 20). RII binding assays reveal that *Drosophila* has about five polypeptides with characteristic features of AKAPs.³ Thus, systematic characterization of the entire constellation of *Drosophila* AKAPs is feasible. Such studies could ultimately yield comprehensive knowledge of regulatory properties, integrative functions and precise physiological roles

* This work was supported by National Institutes of Health (NIH) Grant GM22792 (to C. S. R.) and stipends from NIH Grants GM07260 (to Z. L.) and DK07513 (to E. A. R.). The costs of publication of this article were defrayed in part by the payment of page charges. This article must therefore be hereby marked "advertisement" in accordance with 18 U.S.C. Section 1734 solely to indicate this fact.

The nucleotide sequence(s) reported in this paper has been submitted to the GenBank™/EBI Data Bank with accession number(s) AF132884 and AF132885.

|| To whom correspondence should be addressed: Dept. of Molecular Pharmacology F-229, Albert Einstein College of Medicine, 1300 Morris Park Ave., Bronx, New York 10461. Tel.: 718-430-2505; Fax: 718-430-8922; E-mail: rubin@aecom.yu.edu.

¹ The abbreviations used are: PKA, protein kinase A (cyclic AMP-dependent protein kinase); AKAP, A kinase anchor protein; DAKAP, *Drosophila* A kinase anchor protein; MARCKS, myristoylated alanine-rich C kinase substrate; PSD, phosphorylation site domain; RII, regulatory subunit of type II protein kinase A; RII_{DR}, regulatory subunit of *Drosophila* type II protein kinase A; bp, base pair(s); kbp, kilobase pair(s).

² PKA isoforms are named according to their homodimeric R subunits. Distinct genes encode RII α , RII β , RI α , and RI β .

³ J.-D. Han, Z. Li, and C. S. Rubin, unpublished observations.

of anchored PKA in the context of individual cells of an intact organism.

Recently, we characterized DAKAP550, a large *Drosophila* anchor protein that is asymmetrically positioned in neurons, gut cells, and trachea (13). To further the aim of elucidating the complete spectrum of AKAP structure and function in *Drosophila*, we now report on the characterization of a novel, multi-functional anchor protein named DAKAP200. Differential splicing of DAKAP200 gene transcripts produces a second polypeptide (Δ DAKAP200) that lacks the ability to bind and target PKAII but appears to subserve functions analogous to those of the mammalian myristoylated alanine-rich C kinase substrate (MARCKS) protein.

EXPERIMENTAL PROCEDURES

Screening of cDNA Libraries—Expression libraries of *Drosophila melanogaster* (Canton S strain) cDNAs were searched for inserts encoding A kinase anchor proteins by functional (RII binding) assays and DNA hybridization. cDNA libraries were generated by reverse transcription of mRNAs isolated from embryos 0–24 h after fertilization. Initially, a cDNA library in bacteriophage λ gt11 (CLONTECH) was screened by the procedure of Bregman *et al.* (21). AKAP- β -galactosidase fusion proteins in phage plaques are detected by their ability to bind 32 P-labeled RII β . A 5' *EcoRI*-*XcmI* fragment (386 bp) from the largest cDNA (1.7 kbp) was employed as a template to synthesize a random-primed, 32 P-labeled probe for further screening. Two additional libraries were used: a 5' stretched *Drosophila* embryo cDNA library in bacteriophage λ gt11 (CLONTECH) and a gridded library in the plasmid pNB40 (22, 23). Screening via DNA hybridization (24) yielded 19 independent cDNA clones. Eight of these cDNAs were characterized as described under "Results."

DNA Sequence Analysis—cDNA inserts were subcloned into plasmids pGEM7Z, pGEM5Z (Promega), or pBluescript SKII (Stratagene) and sequenced by a dideoxynucleotide chain termination procedure (25, 26) using T7, T3, SP6, and custom oligonucleotide primers. *Taq* Dye Deoxy Terminator Cycle Sequencing Kits (Applied Biosystems) were used according to the manufacturer's instructions. DNA products were analyzed in a model 377 automated DNA Sequencer (Applied Biosystems) in the DNA Analysis Facility of Albert Einstein College of Medicine.

Computer Analysis—Analysis of sequence data and data base searches were performed using PCGENE-IntelliGenetics software (IntelliGenetics, Mountainview, CA), BLAST programs (27, 28) provided by the NCBI server (National Institutes of Health), and programs provided by the Berkeley *Drosophila* Genome Project server (29).

Assay for RII Binding Activity—Overlay binding assays have been described in several papers (21, 30). In brief, a Western blot is probed with 32 P-labeled RII β (using a subunit concentration of 0.3 nM and 2×10^5 cpm of 32 P radioactivity/ml), and RII β -binding proteins are visualized by autoradiography. Results were quantified by scanning laser densitometry (Amersham Pharmacia Biotech Ultrascan XL laser densitometer) or PhosphorImager analysis (Molecular Dynamics, Inc., Sunnyvale, CA) as described previously (31).

Expression and Purification of a DAKAP200 Fusion Protein—cDNA encoding amino acid residues 475–753 (see Fig. 1) was synthesized via the polymerase chain reaction as described previously (26). The 5' primer contained an *NdeI* restriction site followed by nucleotides 1577–1598 of DAKAP200 cDNA; the 3' primer consisted of the inverse complement of nucleotides 2396–2417 in DAKAP200 cDNA preceded by a *BamHI* restriction site. Product DNA was digested with *NdeI* and *BamHI* and cloned into the bacterial expression plasmid pET-14b (Novagen) that was cleaved with *NdeI* and *BamHI*. The cDNA insert is preceded by vector DNA that encodes a 20-residue N-terminal peptide. This peptide includes six consecutive His residues, which constitute a Ni²⁺-binding site. Fusion gene transcription is driven by the bacteriophage T7 RNA polymerase. *Escherichia coli* BL21 (DE3), which contains a genomic copy of T7 RNA polymerase under control of the *lac* operon, was transformed with recombinant pET14b. Transformed bacteria were grown and induced with isopropyl-1-thio- β -D-galactopyranoside as described previously (32). Bacteria were harvested, disrupted, and separated into soluble and particulate fractions as described in previous studies (32). The partial DAKAP200 fusion protein (designated p-DAKAP70) was recovered in the soluble fraction and was purified to near homogeneity by nickel-chelate chromatography (32). Approximately 3 mg of His₆ fusion protein was obtained from a 300-ml culture of *E. coli*.

Expression and Purification of His-tagged *Drosophila* RII (RII_{DR})—*NdeI* and *BamHI* restriction sites were appended to the 5'- and 3'-ends of cDNA encoding full-length *Drosophila* RII (RII_{DR}). After cloning the cDNA into pET14b, His-tagged RII_{DR} was expressed in *E. coli* and purified to near homogeneity by using the strategy described above for the partial DAKAP200 protein.

Production of Antibodies Directed against DAKAP200—Purified p-DAKAP70 protein (see above) was injected into rabbits (0.35-mg initial injection; 0.2 mg for each of three booster injections) at Covance Laboratories (Vienna, VA) to generate antisera. Serum was collected at 3-week intervals.

Affinity Purification of Anti-RII_{DR} Immunoglobulins—Purified His-tagged RII_{DR} fusion protein was coupled to CNBr-activated Sepharose 4B (Amersham Pharmacia Biotech) (21) to yield a final concentration of 1.5 mg of protein bound per ml of resin. Antiserum (2 ml) generated against murine RII α was incubated with 2 ml of RII_{DR} fusion protein-Sepharose 4B for 2 h at 20 °C. Next, the resin was packed into a column and washed with 20 mM Tris-HCl, pH 7.6, 0.5 M NaCl until the flow-through reached an A₂₈₀ of 0. The column was successively eluted with 5 ml of 0.5% acetic acid, pH 2.5, 0.15 M NaCl, and 5 ml of 0.1 M diethylamine, pH 11.8, to release IgGs. Sufficient 1 M Na₂ HPO₄ or 0.5 M Hepes was added to column fractions to adjust the pH to ~7.5. IgGs were dialyzed against PBS containing 50% glycerol, quantified by absorbance at 280 nm, and stored at -20 °C.

Preparation of Cytosolic and Particulate Proteins from *Drosophila*—*Drosophila* embryos, larvae, pupae, or separated fly heads and bodies were suspended in 4 volumes of buffer A (20 mM sodium phosphate, pH 7.4, 20 mM NaCl, 0.2 mM dithiothreitol, 1 mM EDTA, 0.2 mM EGTA, 10 μ g/ml soybean trypsin inhibitor, 40 μ g/ml aprotinin, 10 μ g/ml pepstatin A, and 40 μ g/ml leupeptin) and were disrupted in a Polytron homogenizer (two 30-s cycles of homogenization at the maximum setting). All operations were performed at 0–4 °C. The homogenate was centrifuged at 12,000 $\times g$ for 20 min, and the supernatant solution (cytosol) was collected. The pellet was resuspended in the original volume of buffer A, homogenized, and centrifuged as described above. The pelleted, particulate fraction of *Drosophila* homogenates was dispersed in the starting volume of buffer A by a final round of homogenization.

Preparation of Cytosolic and Particulate Fractions from *Drosophila* S2 Cells and Hamster AV12 Cells—Cytosolic and particulate proteins were prepared as indicated above, with several modifications. Buffer A was replaced with buffer B (20 mM Hepes-NaOH, pH 7.4, 2 mM DTT, 5 mM EDTA, 1 mM EGTA, 20 mM NaCl, 10 μ g/ml pepstatin A, 20 mM benzamidinium-HCl, 100 μ g/ml pefablock). Cells were disrupted in a Dounce homogenizer (tight) with 50 strokes of the pestle. Centrifugation was performed at 150,000 $\times g$ for 30–60 min.

Electrophoresis of Proteins—Proteins were denatured in gel loading buffer and subjected to electrophoresis in 7.5 or 10% polyacrylamide gels containing 0.1% SDS as described previously (21). Myosin ($M_r = 200,000$), phosphorylase *b* (97,000), transferrin (77,000), albumin (68,000), ovalbumin (45,000), and carbonic anhydrase (29,000) were used as standards for the estimation of M_r values.

Immunoprecipitations—Anti-DAKAP200 serum (2 μ l) was added to samples (300–500 μ g of protein) of cytosolic proteins or Triton X-100 solubilized, membrane proteins from S2 or AV12 cells. After incubation at 4 °C for 16 h, 40 μ l of a 50% suspension of protein A-Sepharose 4B beads was added to the samples. The beads were washed three times with phosphate-buffered saline, incubated 1 h with 5% milk proteins in phosphate-buffered saline, and washed three more times with PBS prior to addition to the sample containing antigen-IgG complexes. After 2 h on ice, beads were recovered by centrifugation at 2000 $\times g$ for 1 min. The resin was then washed (4 °C) three times with 1 ml of phosphate-buffered saline lacking detergent. Finally, the beads were suspended in gel loading buffer and heated for 5 min at 95 °C in preparation for denaturing electrophoresis. The same procedure was used to immunoprecipitate RII_{DR}-DAKAP200 complexes with 4 μ g of affinity-purified anti-RII_{DR} IgGs.

Cell Culture and Transfections—Hamster AV12 cells (derived from a subcutaneous tumor) were obtained from the American Type Culture Collection. Cells were grown at 37 °C in Dulbecco's modified Eagle's medium containing 10% fetal calf serum. *Drosophila* embryo-derived Schneider S2 cells were grown at 27 °C in Schneider's medium containing 10% fetal calf serum.

Full-length cDNA encoding DAKAP200 was excised from plasmid pGEM7Z by digestion with *BamHI* and *XbaI*. The *BamHI* overhang was made blunt with Klenow DNA polymerase prior to digestion with *XbaI*. The cDNA fragment was then cloned into the mammalian expression vector pCIS2 (33), which had been cleaved with *NotI*, blunted, and then cleaved with *XbaI*. This placed DAKAP200 cDNA downstream from a

constitutively active cytomegalovirus promoter and upstream from a polyadenylation signal. AV12 cells were transfected with recombinant pCis2 plasmid via calcium phosphate precipitation (34).

Full-length RII_{DR} cDNA was excised from pGEM5Z by digestion with *Sa*I and *Spe*I. The cDNA fragment was cloned into the *Drosophila* expression plasmid pMK33 HS (generously provided by Dr. Nick Baker, Department of Molecular Genetics, Albert Einstein College of Medicine) that was cleaved with *Xho*I and *Spe*I. This placed the RII_{DR} cDNA downstream from a strong, copper(II)-inducible metallothionein promoter/enhancer and upstream from a polyadenylation signal. pMK33 HS also contains a hygromycin resistance gene that is controlled by a constitutively active *Copia* promoter. S2 cells were transfected by the calcium phosphate-DNA co-precipitation method, and stable transfectants were obtained by growth in 0.3 mg/ml hygromycin for 14 days.

Protein Determination—Protein concentrations were determined with the Coomassie Plus Protein Assay Reagent (Pierce) using bovine albumin as a standard.

Western Immunoblot Analysis—Western blots of cytosolic and particulate proteins from AV12 and S2 cells were blocked, incubated with antiserum, and washed as described previously (35). DAKAP200, ΔDAKAP200, and RII_{DR} polypeptides were visualized by indirect chemiluminescence using an enhanced chemiluminescence (ECL) kit from Amersham Pharmacia Biotech. Membranes were incubated with horseradish peroxidase coupled with goat immunoglobulins directed against rabbit IgG heavy and light chains (Amersham Pharmacia Biotech) in 20 mM Tris-HCl, pH 7.4, containing 0.15 M NaCl and 0.1% (w/v) Tween 20 (10 ml of solution/gel lane) for 90 min at 22 °C. Filters were then washed, incubated with Luminol, and exposed to x-ray film for 2–30 s to record chemiluminescence signals. Relative amounts of proteins were determined by scanning densitometry (31, 35). Standard curves were prepared with 0.5–100 ng of recombinant protein standards. Amounts of protein in experimental samples were obtained from the linear portion of the standard curve.

RESULTS

Discovery of cDNAs Encoding a Novel *Drosophila* AKAP—Candidate cDNA clones for *Drosophila* AKAPs were isolated from an embryo cDNA expression library in bacteriophage λgt11. β-Galactosidase-AKAP fusion proteins in phage plaques were detected by their ability to bind ³²P-labeled RII subunits (21). Twenty-one cDNA clones were isolated from 4 × 10⁵ phage. DNA hybridization analysis revealed that eight cDNAs encoded portions of the previously characterized DAKAP550 protein (13). The cDNA inserts from five distinct, cross-hybridizing clones were ligated into the plasmid pGEM7Z and sequenced. The largest cDNA (1736 bp) contained an open reading frame for 476 codons, a translation stop signal, and 3'-untranslated sequence. Sequences of the smaller cDNAs were included within the 1.7-kbp cDNA. A 5'-stretched *Drosophila* embryo cDNA library in bacteriophage λgt11 and a gridded, high density library in the plasmid pNB40 (22, 23) were screened by DNA hybridization to obtain sequences of upstream codons and the 5'-untranslated region. Nineteen cDNA clones were retrieved from the libraries. Eight nearly full-length or overlapping partial cDNAs were subcloned into pGEM7Z or pBluescript plasmids and sequenced to determine a derived amino acid sequence for an anchor protein named DAKAP200.

The sequence of the largest DAKAP200 cDNA (3053 bp) is deposited in GenBank™ (accession number AF132884). A predicted initiator Met codon (nucleotides 155–157) is incorporated within an optimal translation start motif (ANNATGG, nucleotides 152–158) (36). The putative 154-bp 5'-untranslated portion of the cDNA lacks alternative ATG sequences but includes translation stop codons in all reading frames. In addition, amino acid residues 1–7 constitute an acceptor site for myristoylation (see Fig. 1), a modification that occurs at the N terminus of proteins. An open reading frame of 752 codons follows the initiator ATG and precedes a translation stop signal at nucleotides 2414–2416. The 3'-untranslated region comprises 614 bp and is followed by a polyadenylate tail. Processing of the 3'-end of DAKAP200 mRNA appears to be governed

by either of two overlapping, atypical poly(A) addition signals (GATAAA or AATATA, nucleotides 3004–3014) that precede the polyadenylate tail by 22 or 17 nucleotides.

Several Structural Motifs Are Evident in the Derived Amino Acid Sequence of DAKAP200—DAKAP200 is composed of 753 amino acids and has a calculated *M_r* of 79,075 (Fig. 1). The anchor protein is exceptionally acidic (pI ~3.8) and has an atypical amino acid composition. Glu, Asp, Ser, Thr, Ala, and Pro account for 61% of the residues in DAKAP200. In contrast, Cys, Met, Trp, and Tyr are included at only five positions (0.7% of total amino acids) in the polypeptide chain. DAKAP200 has an apparent *M_r* of 200,000 upon electrophoresis under denaturing conditions (see below). High net negative charge and aberrantly reduced electrophoretic mobility are properties shared between DAKAP200 and mammalian AKAPs (5, 9, 37). Most AKAPs have been assigned names that correspond to their apparent *M_r* values (5, 6). Thus, the name *Drosophila* **A** **k**inase **a**nchor protein of **200** kDa, or DAKAP200, is formulated in accord with standard nomenclature for anchor proteins.

The DAKAP200 sequence is not highly homologous with sequences of previously studied polypeptides. However, several segments of the sequence shown in Fig. 1 provide clues about potential targeting, tethering (RII binding), and regulatory domains. The N terminus of DAKAP200 includes a Gly residue adjacent to the initiator Met and a Ser-Lys dipeptide at positions 6 and 7. This sequence (MGXXXSK) constitutes an optimal target site for the ubiquitous enzyme *N*-myristoyl-CoA transferase (38). A segment of DAKAP200 that encompasses residues 119–148 (Fig. 1) includes a large cluster of Lys residues that create a highly basic (pI ~11.5) and positively charged (+12) domain in the midst of a protein with a predicted overall charge of -116 at pH 7. The compositions of the basic region in DAKAP200 and a central portion of MARCKS and MARCKS-related proteins (MacMARCKS, F52, MRP) (39, 40) are similar, although the degree of amino acid identity is modest (≤30%) when the indicated sequences are aligned. The basic region of MARCKS proteins (named the phosphorylation site domain (PSD)) is a major target for protein kinase C-catalyzed phosphorylation in many mammalian cells (39, 40). The *Drosophila* anchor protein also possesses Pro-rich regions (amino acids 328–332 and 468–479; Fig. 1) that may serve as docking sites for proteins with Src homology 3 domains (41).

Organization and Location of the DAKAP200 Gene—Fragments of genomic DNA that are cloned in P1 vectors are being sequenced and ordered by the Berkeley *Drosophila* Genome Project (29). Screening of the Berkeley *Drosophila* Genome Project Data base with the full-length DAKAP200 cDNA sequence revealed that P1 clone DS02110 (GenBank™ accession number AC004423) contains the DAKAP200 gene as well as complete 5'- and 3'-flanking regions. (No previous studies have analyzed this locus to (a) elucidate the nature and organization of component genes or (b) investigate the expression, properties, and functions of the encoded mRNAs and proteins). Alignment of DAKAP200 cDNA with portions of the DS02110 sequence revealed the organization of the cognate gene. The DAKAP200 structural gene spans 15,220 bp and is composed of six exons and five introns (Table I). The first exon serves as a template for transcription of a short segment of 5'-untranslated mRNA. Exon 1 precedes a large intron (~11 kbp) that accounts for >70% of the nucleotides at this locus. Exons 2–6, which encode the DAKAP200 open reading frame and 3'-untranslated nucleotides in mRNA, contain a total of 2773 bp. Small and medium size introns (introns 2–5, Table I) contribute only 1200 bp of intervening DNA sequence in this region. Exon 5 is atypically large and includes a block of 381 codons that direct the incorporation of ~50% of the constituent amino

acid residues into the DAKAP200 polypeptide. A Pro-rich region and the RII tethering domain are encoded by exon 5 (Fig. 1). *In situ* hybridization assays performed by the Berkeley *Drosophila* Genome Project group disclosed that the anchor protein gene is located on the left arm of chromosome 2 at the cytological position designated 29C3. The DAKAP200 gene lies between genes named *fuzzy* and *gurken* at positions 2–32 on the physical (genome) map. Elucidation of the intron/exon organization of the DAKAP200 gene, as well as complete 5'- and 3'-flanking sequences, provides the first comprehensive picture of an AKAP locus; comparable information is not available for any of the mammalian AKAP genes.

Identification of an RII Binding Site in DAKAP200—An approximate location for the PKAII tethering site in DAKAP200 was established by sequencing five cDNAs that directed synthesis of RII-binding, fusion proteins in plaques of a bacteriophage expression library (see above). The sequence of the smallest cDNA (147 bp) encodes a region of the anchor protein bounded by Asp⁴⁹⁰ and Glu⁵³⁸ (Fig. 1). The same sequence was present in each of the larger (1.1–1.7 kbp) cDNAs. Tethering sites in mammalian AKAPs are composed of ~20 amino acids and contain a precisely spaced group of residues with large, aliphatic side chains (Leu, Val, Ile, and Thr; Fig. 2A) that cooperatively governs sequestration of RII α and RII β subunits (35). Residues 511–530 in DAKAP200 can be aligned with tethering regions of mammalian AKAPs (9, 35, 42), so that Ile⁵¹¹, Ile⁵¹⁸, Val⁵¹⁹, Thr⁵²³, and Val⁵³⁰ are in register with essential hydrophobic residues in previously characterized RII binding sites (Fig. 2A). A final conserved position is occupied by a smaller hydrophobic residue (Ala⁵²⁷) in the *Drosophila* anchor protein. RII binding domains of mammalian AKAPs are predicted to fold as an amphipathic α -helix that contains one markedly hydrophobic surface (43). This feature is also evident in the segment of DAKAP200 that encompasses residues 511–528 (Fig. 2B). Folding algorithms predict that this partial polypeptide is organized into an α -helix in which 9 of 10 side chains on one surface have hydrophobic character (Fig. 2B). Thus, amino acids 511–530 constitute a candidate RII binding site in DAKAP200.

To further characterize the tethering domain, a fragment of DAKAP200 cDNA (nucleotides 1577–2314) that encodes amino acids 475–753 (Fig. 1) was amplified by polymerase chain reaction. The cDNA fragment was cloned into the bacterial expression plasmid pET14b, thereby creating an in-frame fusion with plasmid DNA that encodes a 20-residue N-terminal peptide (see "Experimental Procedures"). The fusion peptide includes six consecutive His residues (His tag) that constitute a high affinity binding site for divalent metals. A substantial amount of soluble, His-tagged, partial DAKAP200 was synthesized in transformed *E. coli* during a 2-h incubation with 1 mM isopropyl-1-thio- β -D-galactopyranoside (Fig. 3A, lane 2). The acidic, recombinant protein exhibited an abnormally large apparent M_r (70,000) during denaturing electrophoresis; the calculated M_r value of the partial DAKAP200 protein is 34,000. The soluble fusion protein (named p-DAKAP70) was purified to near homogeneity by affinity chromatography on Ni²⁺-chelate Sepharose 4B resin (Fig. 3A, lane 3).

Small amounts of immobilized p-DAKAP70 avidly bound ³²P-RII β (human) in an overlay assay performed with a low concentration (0.3 nM) of labeled ligand (Fig. 3B). Similar results were obtained with radiolabeled murine RII α , thereby indicating that the tethering domain of DAKAP200 complexes both RII isoforms with high affinity. Experiments that definitively map N and C-terminal boundaries of the RII binding site and reveal individual amino acids that are essential for high affinity ligation of RII by DAKAP200 are presented in an

```

1  M G K A Q S K R S I D I T T D P K K V G E G D E V A G K V E
31  K I D V D Q K T D A P A V N G D A A T P K E G G D E A A A V
61  E K K E T E E H S E N D K D L T T E K S A A V A E G D D A V
91  A E T A K G E E G S P K E A A A G E D I T P L A D E S I K S
121 K S K K D K V K K K W S F R S I S F G K K D K Q K P A K S E
151 E A T S P T S G T T S P T T A E A E A A P A G D A A V A E P
181 S V A T N G E A E K P A E T A T A T S E P A S K D E K P A E
211 N G S A T E Q E K Q A N G E T E K A A P A P S T V E E A A K
241 P K P A E E P A T V T A T E S N T T A T E E V P V K E S Q P
271 E P E V V T N G H G A G E A L T N G S S N G L A E S P V T E
301 T A P V A D N I P S N V D D E P P H Q N G T N G T T P P P
331 T P V A T E I E K G Q Q I E A S S E V I E T V T P S O A E E
361 E V V A A I I K A V S S E P E A E T E T E T E A E F G F V L V
391 A P V S T E V E V P V P V S I S P I E P V A E V S O V K I E P I
421 V R I P E V E A K S V A D V S E A D T E S V P K V S E L K T
451 E V S E I E F E S V I V E T R S S S P P P P L P K S P P P S
481 R V S A F V L S E D V I E E Q V T P N V P E V N D V K P D E
511 I E Q Q A I S I V A E I T E O A A E I V I T E O E K Q Q E E A
541 K V D S V E E T I E E R S S T V V V E F V L P V Q N D E V T
571 A P S P T P D D V Q K P I E D Q D T P D E K E S Y P V P D P
601 I D P A A V N D E V A V T E A V D C E V E K E T G S I S S N
631 V A E S S S V S D E Q A A I E N O V E T L E F O T V A V E E
661 T T E O E T S D Q Q V I S E E A H S D N D K E N E I D L V E
691 N I I S D L D A P I T K A G G D L L V E L D A R S A E Q E G
721 E S N N K V D L A K D L K E K N A A A A D V T T Q E Q L P V
751 T C E

```

Molecular weight = 79075
pI ~ 3.8

Amino acid composition					
90 A	2 C	4 H	1 M	65 T	
5 R	30 Q	35 I	5 F	1 W	
25 N	127 E	19 L	63 P	1 Y	
49 D	30 G	54 K	68 S	79 V	

FIG. 1. Identification of structural motifs in the DAKAP200 protein that predict specific domain functions. The complete amino acid sequence of DAKAP200 is presented. Residues that constitute a target site for *N*-myristoyl transferase are shown in *boldface type* and *dashed underline* at the N terminus. Three conserved amino acids that ensure a maximal level of myristoylation are marked with *asterisks*. A highly basic, positively charged segment of DAKAP200 (residues 119–148) is depicted in *boldface type*. Two Pro-rich regions are indicated with *boldface italic type*. An RII binding site (residues 511–530) is enclosed in a *rectangle*. The sequence encoded by a large, alternatively spliced exon (exon 5) is marked by a *solid underline* and includes amino acids 345–725. The amino acid composition is shown below the DAKAP200 sequence. Amino acids that are unusually abundant in DAKAP200 are indicated with *boldface type*; residues that are unusually rare are shown in *boldface italic type*. The amino acid sequence of Δ DAKAP200 is obtained by linking residues 1–344 with amino acids 726–753.

TABLE I
Organization of the DAKAP200 gene

Exon	Nucleotides	Amino acid residues	Downstream intron bp
1	125	5'-UT	10,987
2	214	1–61	70
3	396	62–193	60
4	443	194–344	252
5	1144	345–725	818
6	701	726–753 and 3'-UT ^a	

^a UT, untranslated sequence.

accompanying paper (44).

A caveat is that both binding studies and functional screening of cDNA expression libraries were designed and executed on the basis of a logical but unproved assumption, that mammalian RII isoforms are interchangeable substitutes for authentic *Drosophila* RII (RII_{DR}) subunits. To verify this assumption and demonstrate more directly the physiological relevance of the novel fly anchor protein, it was essential to examine the ability of DAKAP200 to bind RII_{DR}. Recently, the Kalderon

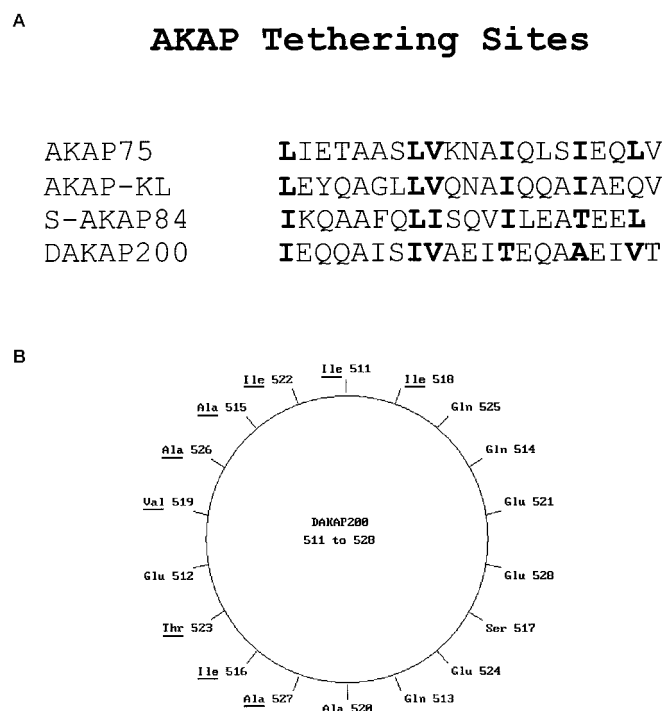


FIG. 2. Identification of a predicted RII binding site in DAKAP200. *A*, six hydrophobic amino acids in a segment of DAKAP200 (residues 511–530) align in register with key hydrophobic residues in the RII tethering domains of AKAP75 (residues 392–413; Ref. 35), S-AKAP84 (residues 306–325; Ref. 9), and AKAP-KL (residues 586–605; Ref. 42). Critical hydrophobic residues are shown in *boldface type*. *B*, a *helical wheel diagram* of the orientation of hydrophobic and hydrophilic amino acids in the RII binding site of DAKAP200. Amino acids that contribute to an extended hydrophobic surface are *underlined*.

laboratory⁴ cloned and sequenced cDNA that encodes the 376-residue RII_{DR} polypeptide. Structural features that govern subunit dimerization and create a docking surface for AKAPs are located near the amino terminus (residues 1–50) of mammalian RII isoforms (32, 45–49). Alignment of the N termini of RII_{DR} and RII α reveals that the two sequences are quite divergent (only 44% identity). However, groups of aromatic residues (Phe and Tyr) and amino acids with large aliphatic side chains (Leu, Val, and Ile) contribute the essential functional properties of dimerization and AKAP binding regions in RII α and RII β (32, 45–49). Amino acids with these characteristics are conserved at all corresponding positions within residues 1–50 of RII_{DR}.

His-tagged RII_{DR} was expressed in *E. coli* by using the strategy outlined above for p-DAKAP70. Approximately 1 mg of nearly homogeneous RII_{DR} (apparent $M_r = 54,000$) was obtained from a 350-ml culture of *E. coli*. Like mammalian RII subunits, RII_{DR} contains the PKA phosphorylation site sequence (RRXSX) in a linker region between the dimerization-AKAP binding domain and the cAMP binding sites. Thus, RII_{DR} was labeled by incubation with Mg- $[\gamma\text{-}^{32}\text{P}]\text{ATP}$ and the catalytic (C) subunit of PKA. ^{32}P -Labeled RII_{DR} binds with low levels of p-DAKAP70 (Fig. 3C, lanes 2–4) and also forms a stable complex with bovine AKAP75 (Fig. 3C, lane 5). Thus, structural features that mediate interactions between RII subunits and AKAPs have co-evolved and are conserved from flies to humans. Binding interactions between RII α , RII β , or RII_{DR} and various AKAPs are sufficiently similar to enable their interchangeable use. Since recombinant mammalian RII isoforms are available in plentiful supply and these proteins are more thoroughly characterized than RII_{DR}, they were em-

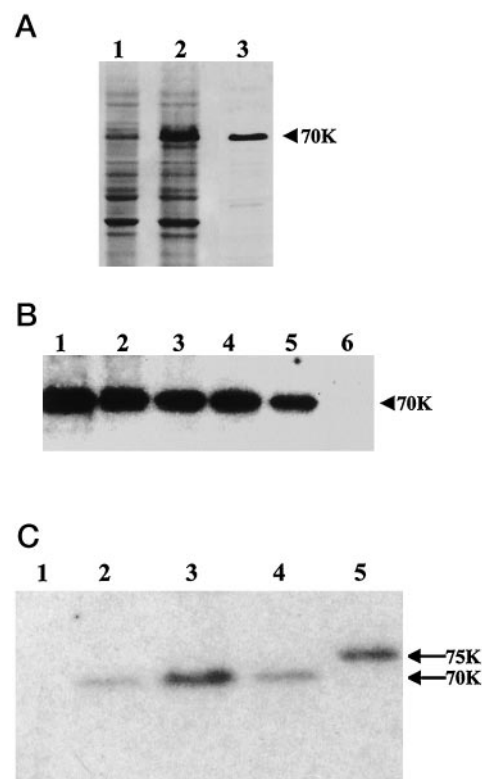


FIG. 3. Expression, purification, and RII binding activity of a DAKAP200 partial protein (p-DAKAP70). *A*, a His-tagged fusion protein that contains residues 475–753 (Fig. 1) of DAKAP200 was expressed in *E. coli* and purified by affinity chromatography as described under “Experimental Procedures” and “Results.” Samples of total soluble protein from transformed and induced *E. coli* (25 μg , lane 2), proteins in the column flow-through (25 μg , lane 1), and protein eluted with 1 M imidazole (1 μg , lane 3) were size-fractionated by denaturing electrophoresis. A 10% polyacrylamide gel that was stained with Coomassie Blue is shown. *B*, Samples of p-DAKAP70 were subjected to electrophoresis in a 0.1% SDS, 10% polyacrylamide gel. Proteins were then transferred to an Immobilon P membrane and incubated with ^{32}P -labeled RII (0.3 nM) (overlay assay, see “Experimental Procedures”) to determine the binding activity of the fusion protein. Lanes 1–6 received 20, 10, 5, 2.5, 1, and 0 ng, respectively, of the partial anchor protein. An autoradiogram is presented. Only the relevant portion of the gel is shown; no other radioactive bands were observed. *C*, a Western blot was prepared using samples of purified p-DAKAP70 and bovine brain AKAP75. The blot was probed with ^{32}P -labeled RII_{DR}. ^{32}P -RII_{DR}·AKAP complexes were visualized by autoradiography. Lanes 2–4 contained 100, 200, and 150 ng, respectively, of p-DAKAP70; lane 5 received 150 ng of AKAP75. Lane 1 was loaded with 1 μg of transferrin ($M_r = 77,000$) and 1 μg albumin ($M_r = 67,000$) and served as a negative control.

ployed for most of the studies presented herein. Repetition of experiments with RII_{DR} yielded similar results in all instances.

Alternative Splicing of DAKAP200 mRNA Produces a Predicted Protein (Δ DAKAP200) That Lacks an RII Tethering Domain—A novel, 1.9-kbp insert was discovered by sequencing candidate DAKAP200 cDNAs obtained from phage and bacterial libraries (see above). The sequence of 5'-untranslated nucleotides and a large contiguous DNA segment comprising 344 codons was identical with nucleotides 94–1186 in DAKAP200 cDNA (GenBankTM accession number AF132884). However, nucleotide 1186 was directly linked to a 3' sequence that matches perfectly with nucleotides 2330–2964 in DAKAP200 cDNA. Alignment of the 1.9-kbp cDNA (GenBankTM accession number AF132885) and DAKAP200 gene sequences revealed that the smaller cDNA was produced by the precise excision of exon 5 (Table I) from the DAKAP200 transcript. The shorter cDNA and its cognate polypeptide were named “*deleted DAKAP200*,” or Δ DAKAP200, to indicate their

⁴ D. Kalderon, unpublished results.

derivation from DAKAP200 via exon elimination. Excision of exon 5 results in the loss of a block of 381 residues that includes the RII binding region and a Pro-rich sequence that is a candidate Src homology 3 binding site. Other structural features of DAKAP200 are retained in the 372-residue Δ DAKAP200 polypeptide (Fig. 1). Δ DAKAP200 is a highly acidic protein (pI \sim 4.2) in which Glu, Asp, Ala, Pro, Ser, and Thr contribute 62% of total amino acids. The protein lacks Tyr, whereas Met, Cys, and Trp appear only once in the conceptual translation of the protein (Fig. 1). Δ DAKAP200 has a calculated M_r of 38,000, but its atypical migration in denaturing electrophoresis yields an apparent M_r of 95,000 (see below). Moreover, the N-terminal myristoylation site (residues 1–7), the highly basic PSD-like region (residues 118–148), and a Pro-rich (and Thr-rich) segment (residues 316–335) are present in both Δ DAKAP200 and the larger DAKAP200 isoform.

DAKAP200 and Δ DAKAP200 Are Expressed throughout *Drosophila* Development and in an Embryo-derived Cell Line—The purified 279-residue protein fragment corresponding to the central and C-terminal portion of DAKAP200 (amino acids 475–753, p-DAKAP70; Fig. 1) was injected into rabbits to produce antibodies. A high dilution (1:3000) of antiserum yielded robust signals on lanes of a Western blot that contained low levels of partial DAKAP200 protein (Fig. 4A). Thus, anti-DAKAP200 IgGs bind with high affinity and provide a sensitive assay for monitoring expression of the *Drosophila* anchor protein.

The apparent M_r of the polypeptide encoded by full-length DAKAP200 cDNA was determined by a transfection/expression experiment. A cDNA insert containing the complete anchor protein open reading frame was ligated into the multiple cloning site of mammalian expression vector pCIS2 (see "Experimental Procedures"). Recombinant vector was introduced into a hamster tumor cell line (AV12) as a calcium phosphate-DNA co-precipitate (37). A protein with an apparent M_r of 200,000 was detected by anti-DAKAP200 IgGs in both the cytosolic and particulate fractions of AV12 cells that contained the transgene (Fig. 4B, lanes 1 and 2). A slightly smaller immunoreactive band ($M_r \sim$ 195,000) was also evident in the pellet fraction. These proteins were not detected in cytosol and particulate fractions isolated from nontransfected AV12 cells (Fig. 4B, lanes 3 and 4). No signals were obtained when lanes 1 and 2 were duplicated and probed with preimmune serum (Fig. 4B, lanes 5 and 6) or immune serum in the presence of excess ($3 \mu\text{g}$) antigen (Fig. 4B, lanes 7 and 8). Thus, the antibodies are highly specific and indicate that the 3-kbp DAKAP200 cDNA directs synthesis of a 753-residue protein (Fig. 1) with an unexpectedly large apparent M_r (\sim 200,000). The appearance of a DAKAP200 doublet (Fig. 4B, lane 2) suggests that the anchor protein may be a target for post-translational modification and/or proteolytic cleavage.

An embryo-derived *Drosophila* cell line named Schneider S2 cells (hereafter designated "S2 cells") expresses endogenous DAKAP200 that is visualized as a cluster of three or four polypeptide bands with apparent M_r values in the range of 190,000–205,000 (Fig. 4C, lanes 1 and 2). The intensity of the smallest of these bands varies widely among samples and may arise from proteolysis or dephosphorylation. In contrast, the 200/205-kDa doublet reproducibly accounts for the bulk of the anchor protein. Anti-DAKAP200 IgGs also bind with a protein that exhibits an apparent M_r of 95,000 (Fig. 4C, lanes 1 and 2). Together, highly specific IgG binding (Fig. 4C, compare lanes 1 and 2 with lanes 3–6) and the size of the protein (*i.e.* \sim 50% of apparent M_r of DAKAP200) suggest that the 95-kDa band corresponds to the 372-residue Δ DAKAP200 polypeptide (Fig. 1). The 95-kDa protein is detected by the IgGs because 28

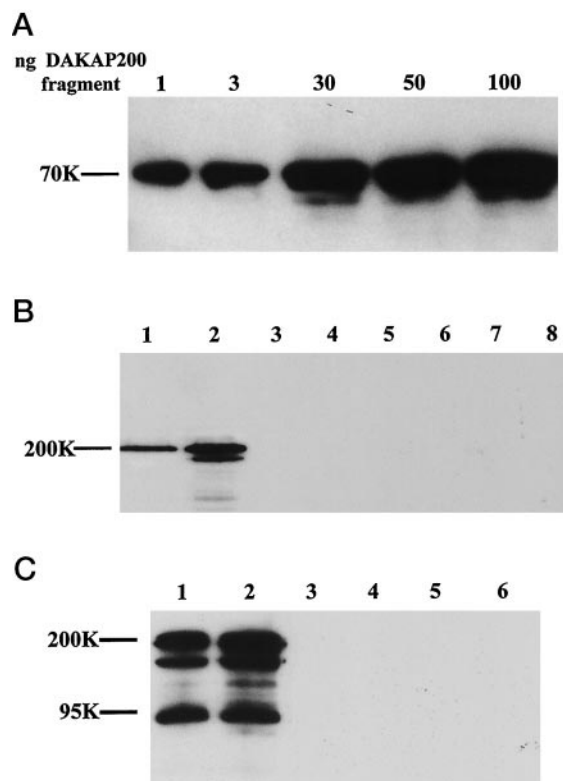


FIG. 4. Anti-DAKAP200 IgGs avidly bind recombinant anchor protein synthesized in bacteria, mammalian cells, and *Drosophila* S2 cells. *A*, a Western blot was prepared from a denaturing 10% polyacrylamide gel as described under "Experimental Procedures." The lanes were loaded with the indicated amounts of partial DAKAP200 (p-DAKAP70). The blot was probed sequentially with anti-DAKAP200 serum (1:3000) and peroxidase-coupled secondary antibodies directed against rabbit IgGs. p-DAKAP70-IgG complexes were visualized by an enhanced chemiluminescence procedure (see "Experimental Procedures"). *B*, hamster AV12 cells were stably transfected with a full-length DAKAP200 transgene as described under "Experimental Procedures." Samples ($30 \mu\text{g}$) of cytosolic (lanes 1, 5, and 7) and total particulate proteins (lanes 2, 6, and 8) were isolated from AV12 cells (see "Experimental Procedures") transfected with the DAKAP200 transgene. Proteins were then size-fractionated by SDS-PAGE (7.5% gel) and transferred to an Immobilon P membrane. Samples ($30 \mu\text{g}$) of cytosolic (lane 3) and particulate (lane 4) proteins from nontransfected AV12 cells were processed in the same manner. Lanes 1–4 were probed with anti-DAKAP200 serum (1:3000); lanes 7 and 8 were incubated with anti-DAKAP200 serum (1:3000) in the presence of $3 \mu\text{g}$ of p-DAKAP70 antigen; and lanes 5 and 6 were incubated with preimmune serum (1:1500). After incubation with secondary antibodies coupled to peroxidase, DAKAP200-IgG complexes were detected by an enhanced chemiluminescence procedure. Signals recorded on x-ray film are shown. Only the relevant portion of the blot is shown. No other immunoreactive proteins were observed. *C*, cytosolic and total particulate fractions were prepared from embryo-derived S2 cells as described under "Experimental Procedures." Samples ($20 \mu\text{g}$) of cytosolic (lanes 1, 3, and 5) and particulate (lanes 2, 4, and 6) proteins were fractionated in an SDS-7.5% polyacrylamide gel and transferred to an Immobilon P membrane. Lanes 1 and 2 were probed with anti-DAKAP200 serum (1:3000); lanes 3 and 4 were incubated with anti-DAKAP200 serum (1:3000) in the presence of excess antigen ($3 \mu\text{g}$ p-DAKAP70); lanes 5 and 6 were exposed to preimmune serum (1:3000). DAKAP200-IgG and Δ DAKAP200-IgG complexes were detected and recorded as described for *B*.

amino acids at the C terminus of the p-DAKAP70 antigen are shared by DAKAP200 and Δ DAKAP200 (Fig. 1). This segment of the anchor protein provides a common epitope(s) that is recognized by anti-DAKAP200 IgGs in the absence of the remainder of the polypeptide.⁵ As expected, expression of the 1.9-kbp Δ DAKAP200 cDNA in AV12 cells elicits accumulation

⁵ H. Feng, Z. Li, and C. S. Rubin, unpublished observations.

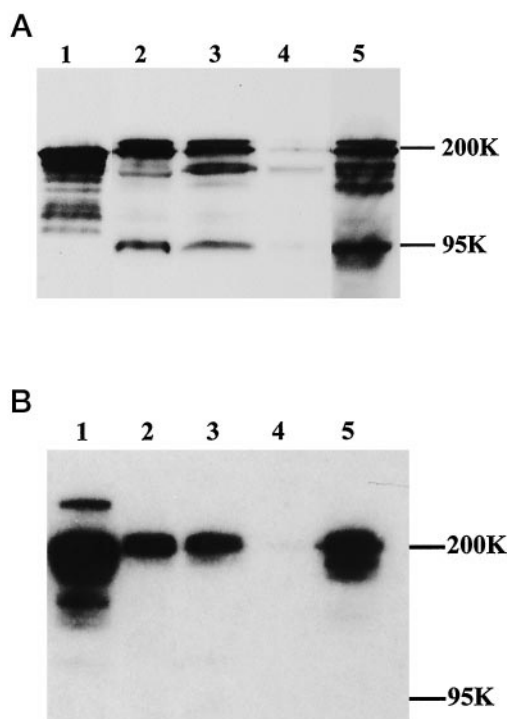


FIG. 5. Antibodies directed against DAKAP200 efficiently precipitate the fly anchor protein and Δ DAKAP95; DAKAP200 accounts for all of the RII binding activity in S2 cells. A, a Western blot was prepared, probed, and developed as described under "Experimental Procedures." Lane 1 received 50 μ g of cytosolic proteins derived from AV12 cells transfected with the DAKAP200 transgene (positive control). Lane 2 contained 50 μ g of cytosolic proteins from S2 cells; lane 3 received 50 μ g of particulate proteins from S2 cells. Anti-DAKAP200 serum (1.5 μ l) was added to 0.25 ml of S2 cytosol (300 μ g of protein). After 16 h at 4 $^{\circ}$ C, antigen-antibody complexes were harvested by the addition of protein A-Sepharose 4B and centrifugation. Precipitated proteins were applied to lane 5. A sample of nonprecipitated proteins in the supernatant solution (20% of total sample) was placed in lane 4. Signals from the ECL assay were recorded on x-ray film. Only the relevant portion of the gel is shown. No other bands were observed on the blot. B, blots were prepared as described above. The identity and amounts of samples applied to lanes 1-5 are the same as described for A. The blot was incubated to equilibrium with 0.3 nM 32 P-labeled RII β (overlay assay, see "Experimental Procedures") to identify AKAPs. An autoradiogram is shown. Antibodies directed against DAKAP200 precipitated essentially all of the RII tethering activity (lane 5) originally observed in S2 cytosol (lane 2). Depletion of the AKAP from cytosol is documented in lane 4. Cytosol from transfected AV12 cells contains recombinant DAKAP200 (positive control) as well as an endogenous mammalian, RII-binding protein (M_r ~260,000) (lane 1).

of a recombinant protein with an apparent M_r of 95,000 (data not shown).

DAKAP200 and Δ DAKAP200 (95 kDa) proteins are distributed nearly equally between cytosolic and total particulate fractions derived from S2 cell homogenates (Fig. 5A, lanes 2 and 3). Cytosolic and particulate RII binding activity was associated exclusively with a tight cluster of proteins that exhibit an apparent M_r of ~200,000 (Fig. 5B, lanes 2 and 3). To determine the relative contribution of DAKAP200 to this tethering activity, cytosol was incubated with antibodies directed against the anchor protein for 16 h. Immune complexes were harvested with protein A-Sepharose 4B beads and assayed via Western blot and overlay binding procedures. Essentially all immunoreactive proteins (200-kDa cluster and 95-kDa band) were depleted from cytosol by immunoprecipitation (Fig. 5A, lane 4). DAKAP200 and Δ DAKAP200 proteins were recovered in high yield in the immunoprecipitate (Fig. 5A, lane 5). Some of the larger polypeptides appeared to be partly degraded during the 16-h incubation used for immunoprecipitation, whereas the

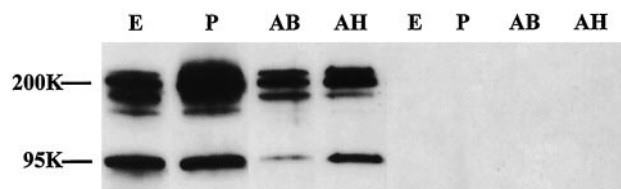


FIG. 6. DAKAP200 and Δ DAKAP200 are expressed at all stages of *Drosophila* development. Cytosol was isolated from embryos (E), larvae (not shown), and pupae (P) as well as the bodies (AB) and heads (AH) of adult flies (see "Experimental Procedures"). Proteins (25 μ g) were size-fractionated by SDS-PAGE (7.5% gel), transferred to a polyvinylidene difluoride membrane, and probed with anti-DAKAP200 serum (1:3000). Immunoreactive proteins were visualized by indirect, enhanced chemiluminescence methodology. The four lanes shown on the left were replicated and incubated with anti-DAKAP200 serum in the presence of excess antigen (3 μ g). No signals were observed (four lanes on the right).

95-kDa Δ DAKAP200 protein was evidently less susceptible to proteolysis. Virtually 100% of RII binding activity was co-isolated with DAKAP200 proteins in the immunoprecipitate (Fig. 5B, lanes 4 and 5). No RII tethering activity was associated with Δ DAKAP200 (Fig. 5, compare A, lanes 2 and 5, with B, lanes 2 and 5) or distinct 200-kDa proteins that co-migrate with DAKAP200 (Fig. 5B, lane 4). These results were replicated when detergent-soluble proteins from the particulate fraction of S2 cells were analyzed by immunoprecipitation and overlay binding assays (data not shown). Thus, the predicted DAKAP200 protein (Fig. 1) is produced endogenously in *Drosophila* embryo cells. Authentic DAKAP200 binds RII subunits with high affinity and appears to be the principal (perhaps only) anchor protein in S2 cells.

Overall patterns of *in vivo* expression of DAKAP200 and Δ DAKAP200 were established by performing Western blot analysis on protein samples isolated from flies at various developmental stages. Results obtained for cytosolic (Fig. 6) and detergent-solubilized, particulate proteins were similar. The DAKAP200 protein cluster was enriched in pupae (3-4-fold higher than other stages) (Fig. 6), but substantial levels of these anchor proteins were also evident in embryos, adults, and larvae (Fig. 6, larvae not shown). Δ DAKAP200 is also detected at all phases of the *Drosophila* life cycle (Fig. 6). This indicates that alternative splicing of DAKAP200 gene transcripts is operative during the progression of embryonic and postembryonic development. The concentration of Δ DAKAP200 in the adult head, which is enriched in neurons, is ~7-fold higher than that observed in body parts (Fig. 6). Therefore, alternative excision of exon 5 from DAKAP200 mRNA and/or stability of Δ DAKAP200 protein may be differentially regulated in a cell/tissue specific fashion in mature *Drosophila*.

A critical test of the idea that the *Drosophila* anchor protein mediates physiologically relevant targeting/immobilization of PKAII *in situ* involves isolation of stable RII-DAKAP200 complexes from intact cells. S2 cells accumulate DAKAP200 (Fig. 5), but contain an extremely low level of endogenous RII_{DR} (data not shown). Therefore, cDNA encoding the complete amino acid sequence of RII_{DR} was inserted into the multiple cloning region of a *Drosophila* expression plasmid pMK33/HS. This positions the 5'-end of the insert downstream from a *Drosophila* metallothionein promoter/enhancer sequence; the 3'-end of RII_{DR} cDNA is followed by a poly(A) addition signal from an actin gene. Moreover, the plasmid contains a hygromycin resistance gene under the control of a strong constitutively active promoter (*Copia* LTR) that enables drug-based selection of stably transfected cell lines. The fly metallothionein promoter is tightly regulated and exhibits little activity in the absence of Cu²⁺ ions. The addition of 0.5-1 mM CuSO₄ to the medium efficiently activates transactivating factors that

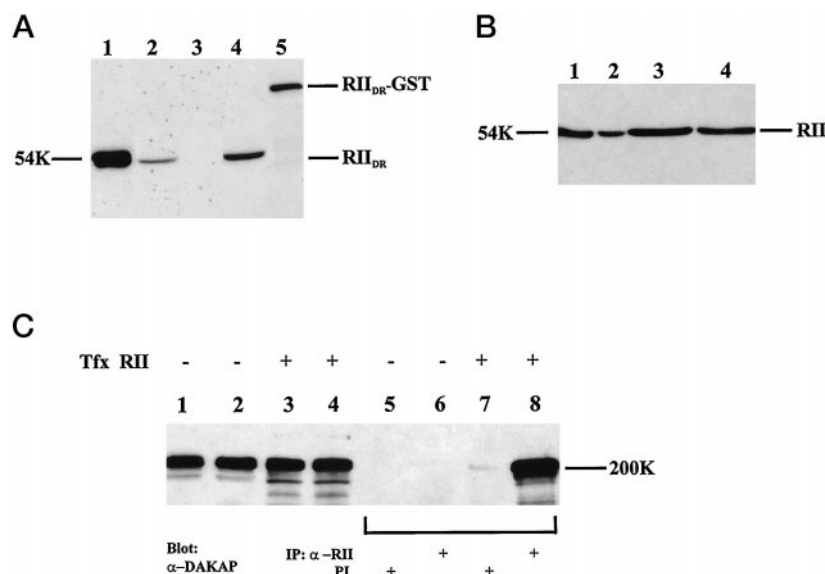


FIG. 7. Affinity-purified anti-mouse RII α IgGs bind *Drosophila* RII; DAKAP200 avidly binds RII_{DR} in intact *Drosophila* cells. *A*, a Western blot analysis was performed with IgG (1 μ g/ml) that was purified on a column of RII_{DR}-Sepharose 6B. Electrophoresis, blotting, incubation with IgG, and the ECL procedure were carried out as described under "Experimental Procedures." Lane 1 contained 250 ng of His-tagged RII_{DR}; samples (30 μ g) of cytosolic proteins from adult *Drosophila*, S2 cells and S2 cells expressing an RII_{DR} transgene were assayed in lanes 2–4, respectively; lane 5 contained 50 ng of a glutathione *S*-transferase-RII_{DR} fusion protein. *B*, samples (50 μ g) of cytosolic (lanes 1 and 3) and particulate (lanes 2 and 4) proteins from two lines of S2 transfectants (which carry the RII_{DR} transgene) were size-fractionated in a denaturing (10%) gel. Cells were induced by incubation with 1 mM CuSO₄ for 16 h prior to lysis. Accumulation of the regulatory subunit of *Drosophila* PKAII was assessed by Western immunoblot analysis. *C*, Western immunoblot analysis was performed as described under "Experimental Procedures." Samples (30 μ g of protein) of cytosol from control S2 cells and S2 cells carrying the RII_{DR} transgene (*Tfx RII*) were assayed in lanes 1 and 3, respectively. Particulate proteins (30 μ g) from control and transfected S2 cells were applied to lanes 2 and 4, respectively. Transfected cells were incubated with 1 mM CuSO₄ for 16 h prior to lysis. Cytosol (300 μ l, 500 μ g of protein) from either control S2 cells or S2 cells transfected with RII_{DR} was mixed with 4 μ g of affinity-purified anti-RII_{DR} IgGs or an equal amount of preimmune (PI) IgG and incubated overnight. Antigen-IgG complexes were harvested with protein A Sepharose 6B and washed as described under "Experimental Procedures." Proteins precipitated from control and transfected cells by preimmune IgGs were analyzed in lanes 5 and 7, respectively. Proteins precipitated from control and transfected S2 cells by anti-RII_{DR} IgGs were analyzed in lanes 6 and 8, respectively. The blot was probed with anti-DAKAP200 serum (1:3000).

potently promote transcription of the chimeric gene. Stable lines of S2 cells that carry the RII_{DR} transgene were established by calcium phosphate-mediated transfection and growth for 14 days in the presence of 0.3 mg/ml hygromycin.

Antibodies initially directed against murine RII α were affinity-purified on a column of His-tagged RII_{DR}-Sepharose 4B (see "Experimental Procedures"). The purified IgGs bound both (His)₆-RII_{DR} and glutathione *S*-transferase-RII_{DR} recombinant fusion proteins on a Western blot (Fig. 7A, lanes 1 and 5). Thus, the antibodies recognized and complexed epitopes within RII_{DR} in addition to (or instead of) the artificial 20-residue His₆ fusion peptide that was appended to the original RII α antigen. No immunoreactive polypeptides were evident among cytosolic proteins isolated from nontransfected S2 cells (Fig. 7A, lane 3). In contrast, affinity-purified IgGs bound a 54-kDa protein in cytosol prepared from S2 cells that were transfected with the RII_{DR} transgene and induced with 1 mM CuSO₄ (Fig. 7A, lane 4). Moreover, cytosol derived from adult *Drosophila* also contained a single immunoreactive protein with an apparent M_r of 54,000 (Fig. 7A, lane 2). The M_r observed for RII_{DR} in S2 cells and intact flies is the same as that previously reported for a near homogenous preparation of the R subunit of *Drosophila* PKAII (19). Similar results were obtained for RII_{DR} associated with the particulate fractions of adult *Drosophila* and transfected S2 cells (data not shown). The blot shown in Fig. 7A was duplicated and probed with anti-RII_{DR} IgGs in the presence of excess highly purified RII_{DR}. No signals were observed under these conditions. Thus, a subset of antibodies directed against mammalian RII α selectively and specifically complex RII_{DR} in extracts of *Drosophila* cells and tissues.

In Situ Generation of DAKAP200-RII_{DR} Complexes—Formation of complexes was investigated in cloned S2 cell lines that were stably transfected with the inducible RII_{DR} transgene.

Similar amounts of RII_{DR} accumulated in the cytosolic and particulate fractions upon incubation of the various cloned cell lines with CuSO₄. Results from two representative S2 transfectants are presented in Fig. 7B. Expression of RII_{DR} subunits did not affect the levels or intracellular distribution of the DAKAP200 protein (Fig. 7C, lanes 1–4). However, after induction of RII_{DR} with Cu²⁺ (Fig. 7C), affinity-purified anti-RII_{DR} IgGs mediated precipitation of a substantial amount of DAKAP200 (Fig. 7C, lane 8). These antibodies failed to precipitate the anchor protein in the absence of RII_{DR} (Fig. 7C, lane 6). The inability of preimmune IgGs to bind the complex (Fig. 7C, lane 7) confirms the specificity of the methodology. DAKAP200 avidly sequesters RII_{DR} in the milieu of intact *Drosophila* cells and produces a complex that is highly stable during immunoisolation and extensive washing. The results support the concept that DAKAP200 and *Drosophila* PKAII can engage in physiologically significant interactions.

DISCUSSION

Complementary DNAs encoding a novel *Drosophila* AKAP (DAKAP200) were discovered by screening expression libraries for high affinity RII-binding proteins. The predicted anchor protein (753 amino acids) has a calculated M_r of 79,075. However, DAKAP200 exhibits an apparent M_r of ~200,000 in SDS-polyacrylamide gels. This discrepancy is probably due to the exceptionally acidic character (pI ~3.8) of the PKAII tethering protein. A high level of net negative charge (–116 at pH 7) apparently reduces SDS binding and promotes retention of higher order structure under conditions that are fully denaturing for more typical proteins. Previously characterized AKAPs are also acidic proteins that display aberrantly large M_r values during denaturing electrophoresis (5, 6, 9, 10, 42). Conservation of a high level of negative charge among *Drosophila*, *Cae*

norhabditis elegans, and mammalian AKAPs suggests that this electrostatic property may play a role in targeting, stabilizing, or immobilizing anchor protein-PKA complexes.

Binding of RII at tethering sites in AKAPs is governed by hydrophobic interactions (35, 42). Structural features and RII binding assays suggest that amino acids 511–530 in DAKAP200 constitute an RII binding site. However, amino acid sequences of tethering domains from DAKAP200 and mammalian anchor proteins are only 20–33% identical. Ligation of RII β , RII α , and RII_{DR} by DAKAP200 is explained by conservation of higher order structure. Like tethering sites in mammalian AKAPs (5, 6, 50), the candidate DAKAP200 RII binding domain is predicted to fold into an amphipathic α -helix with opposing hydrophobic and hydrophilic surfaces (Fig. 2). Five amino acids with bulky, aliphatic side chains (Ile⁵¹¹, Ile⁵¹⁹, Val⁵²⁰, Thr⁵²³, and Val⁵³⁰) in the putative DAKAP200 tethering region align in register with Ile, Val, Thr, or Leu residues in RII binding sites of mammalian AKAPs (Fig. 2). These side chains create a large hydrophobic surface that docks with a complementary apolar surface that is exposed at the N terminus of RII subunits (32, 45–47). Strong evolutionary selection pressure has evidently been exerted on RII tethering modules to retain a configuration of hydrophobic residues that supports highly selective complex (AKAP-RII) formation. Conservation of this structural module and binding mechanism in organisms as diverse as insects and humans suggests that RII tethering sites in AKAPs subserve fundamentally important physiological functions in eukaryotes.

The physiological relevance of DAKAP200 was investigated by testing the ability of the anchor protein to bind an endogenous ligand, RII_{DR}. The RII_{DR} polypeptide sequence contains the hallmarks of classical RII isoforms (55% identical with RII α) but shares little homology with RI α (~28% identity).⁴ DAKAP200 and AKAP75 sequestered radiolabeled RII_{DR} *in vitro*. Thus, RII_{DR} contains the hydrophobic docking region that binds the conserved PKAII tethering module in AKAPs. In addition, anti-RII_{DR} IgGs precipitated a DAKAP200-RII_{DR} complex from S2 cell cytosol. Therefore, DAKAP200 encounters and tightly binds RII_{DR} subunits in intact *Drosophila* cells.

Several domains in DAKAP200 may contribute to the targeting of tethered PKAII. Two Pro-rich regions (residues 328–332 and 468–479) are potential binding sites for cytoskeleton/organelle-associated proteins that contain Src homology 3 domains (41). Amino acids 2–7 (Fig. 1) constitute an acceptor site for *N*-myristoyltransferase. Myristoylation of DAKAP200 would provide a long saturated aliphatic chain that inserts into the hydrocarbon interior of phospholipid bilayers (51, 52). A segment of DAKAP200 (residues 118–148) includes a PSD-like cluster of 13 Lys, five Ser, and five large hydrophobic residues. Positive charge in PSD2S promotes electrostatic binding with negatively charged head groups of membrane phospholipids (53–56). Intercalation of PSD hydrophobic side chains into the apolar interior of a bilayer further stabilizes association of PSD-containing proteins with membranes. N-terminal myristate and a PSD are critical features of MARCKS proteins, which mediate interactions between plasma membrane and F-actin (39, 40, 51–56). The MARCKS PSD is phosphorylated *in situ* by diacylglycerol-activated protein kinase C isoforms (39, 40, 51). Phosphorylation inhibits binding with membrane phospholipids, enables translocation of MARCKS from cell surface to cytoplasm, and promotes cytoskeleton remodeling (51–58). The nonphosphorylated PSD sequesters calmodulin in a calcium-dependent manner (52, 56, 57). Binding of Ca²⁺-calmodulin diminishes the ability of MARCKS to cross-link and bundle actin filaments (57). By analogy, the fly anchor protein may be involved in integrating signals propagated by three

critical second messenger molecules: cAMP, diacylglycerol, and calcium. Moreover, the PSD region of DAKAP200 may enable phosphorylation-controlled shuttling of tethered PKA between two or more intracellular sites.

A novel 1.9-kbp cDNA encodes a second product (Δ DAKAP200) of the anchor protein gene. Δ DAKAP200 is composed of 372 amino acids (calculated $M_r = 38,000$). Messenger RNA encoding the smaller protein is derived from DAKAP200 transcripts by alternative excision of exon 5 (381 codons). Since exon 5 encodes the RII tethering region, Δ DAKAP200 will not anchor PKAII to intracellular sites. Elimination of a Pro-rich region encoded by exon 5 may also preclude Src homology 3 domain-mediated binding with protein ligands and result in the routing of Δ DAKAP200 and DAKAP200-RII complexes to distinct intracellular destinations. It is possible to speculate that a primordial Δ DAKAP200 gene was converted to a modern DAKAP200 gene by insertion of a new exon (“exon shuffling”) that originally encoded a distinct RII binding protein comprising 381 amino acids. If downstream effector/substrates for PKA co-clustered at docking sites for Δ DAKAP200, then substantial selection pressure would have favored retention of the “foreign” exon in the mutant gene. The large size of exon 5 raises the possibility that it arose from reverse transcription of fully processed mRNA.

DAKAP200 and Δ DAKAP200 are synthesized in embryo-derived S2 cells and at all stages of *Drosophila* development. Apparently, both proteins play important physiological roles throughout the life span of the fly. Since the sequence of Δ DAKAP200 is included within DAKAP200, it is probable that these proteins subserve partially overlapping functions. However, exon 5 provides novel amino acid sequences and domains that adapt DAKAP200 for distinct physiological roles (*e.g.* PKAII targeting). The more compact Δ DAKAP200 polypeptide may (a) adopt an alternative folding pattern in one or more domains that mediate unique functions (*e.g.* across the junction encoded by exons 4 and 6); (b) undergo targeting to organelles or regions of cytoskeleton that differ from the destinations reached by DAKAP200-PKAII complexes, and/or (c) subserve functions redundant with those mediated by DAKAP200 in order to ensure proper regulation of critical aspects of homeostasis. Enrichment of Δ DAKAP200 protein in adult head (brain) relative to other body parts (Fig. 6) suggests that a post-transcriptional mechanism might control (in part) targeting of signals along the cAMP/PKA pathway. This mechanism would involve the regulated enhancement or suppression of the excision of an exon during pre-mRNA processing.

Acknowledgment—We thank Ann Marie Alba for expert secretarial assistance.

REFERENCES

- Edelman, A. M., Blumenthal, D. K., and Krebs, E. G. (1987) *Annu. Rev. Biochem.* **56**, 567–613
- Taylor, S. S., Buechler, J. A., and Yonemoto, W. (1990) *Annu. Rev. Biochem.* **59**, 971–1005
- Francis, S. H., and Corbin, J. D. (1994) *Annu. Rev. Physiol.* **56**, 237–272
- Beebe, S. J. (1994) *Semin. Cancer Biol.* **5**, 285–294
- Rubin, C. S. (1994) *Biochim. Biophys. Acta* **1224**, 467–479
- Scott, J. D., and McCartney, S. (1994) *Mol. Endocrinol.* **8**, 5–11
- Faux, M. C., and Scott, J. D. (1996) *Cell* **85**, 9–12
- Gray, P. C., Scott, J. D., and Catterall, W. A. (1998) *Curr. Opin. Neurobiol.* **8**, 330–334
- Chen, Q., Lin, R. Y., and Rubin, C. S. (1997) *J. Biol. Chem.* **272**, 15247–15257
- Lester, L. B., Coghlan, V. M., Nauert, B., and Scott, J. D. (1996) *J. Biol. Chem.* **271**, 9460–9465
- Feliciello, A., Rubin, C. S., Avvedimento, E. V., and Gottesman, M. E. (1998) *J. Biol. Chem.* **273**, 23361–23366
- Miklos, G. L., and Rubin, G. M. (1996) *Cell* **86**, 521–529
- Han, J. D., Baker, N. E., and Rubin, C. S. (1997) *J. Biol. Chem.* **272**, 26611–26619
- Perrimon, N. (1995) *Cell* **80**, 517–520
- Perrimon, N. (1996) *Cell* **86**, 513–516
- Li, W., Ohlmeyer, J. T., Lane, M. E., and Kalderon, D. (1995) *Cell* **80**, 553–562
- Lane, M. E., and Kalderon, D. (1995) *Mech. Dev.* **49**, 191–200

18. Lane, M. E., and Kalderon, D. (1994) *Genes Dev.* **8**, 2986–2995
19. Foster, J. L., Guttman, J. J., Hall, L. M., and Rosen, O. M. (1984) *J. Biol. Chem.* **259**, 13049–13055
20. Kalderon, D., and Rubin, G. M. (1988) *Genes Dev.* **2**, 1539–1556
21. Bregman, D. B., Bhattacharyya, N., and Rubin, C. S. (1989) *J. Biol. Chem.* **264**, 4648–4656
22. Brown, N. H., and Kafatos, F. C. (1988) *J. Mol. Biol.* **203**, 425–437
23. Hoheisel, J. D., Lennon, G. G., Zehetner, G., and Lehrach, H. (1991) *J. Mol. Biol.* **220**, 903–914
24. Lu, X. Y., Gross, R. E., Bagchi, S., and Rubin, C. S. (1990) *J. Biol. Chem.* **265**, 3293–3303
25. Sanger, F., Nicklen, S., and Coulson, A. R. (1977) *Proc. Natl. Acad. Sci. U. S. A.* **74**, 5463–5467
26. Hu, E., and Rubin, C. S. (1990) *J. Biol. Chem.* **265**, 5072–5080
27. Pearson, W. R., and Lipman, D. J. (1988) *Proc. Natl. Acad. Sci. U. S. A.* **85**, 2444–2448
28. Altschul, S. F., Gish, W., Miller, W., Myers, E. W., and Lipman, D. J. (1990) *J. Mol. Biol.* **215**, 403–410
29. Spradling, A. C., Stern, D. M., Kiss, I., Roote, J., Laverty, T., and Rubin, G. M. (1995) *Proc. Natl. Acad. Sci. U. S. A.* **92**, 10824–10830
30. Bregman, D. B., Hirsch, A. H., and Rubin, C. S. (1991) *J. Biol. Chem.* **266**, 7207–7213
31. Ndubuka, C., Li, Y., and Rubin, C. S. (1993) *J. Biol. Chem.* **268**, 7621–7624
32. Li, Y., and Rubin, C. S. (1995) *J. Biol. Chem.* **270**, 1935–1944
33. Gorman, C. M. (1990) *Curr. Opin. Biotechnol.* **1**, 36–47
34. Li, Y., Ndubuka, C., and Rubin, C. S. (1996) *J. Biol. Chem.* **271**, 16862–16869
35. Glantz, S. B., Li, Y., and Rubin, C. S. (1993) *J. Biol. Chem.* **268**, 12796–12804
36. Kozak, M. (1987) *Nucleic Acids Res.* **15**, 8125–8148
37. Hirsch, A. H., Glantz, S. B., Li, Y., You, Y., and Rubin, C. S. (1992) *J. Biol. Chem.* **267**, 2131–2134
38. Johnson, D. R., Bhatnagar, R. S., Knoll, L. J., and Gordon, J. I. (1994) *Annu. Rev. Biochem.* **63**, 869–914
39. Aderem, A. (1992) *Cell* **71**, 713–716
40. Blackshear, P. J. (1993) *J. Biol. Chem.* **268**, 1501–1504
41. Cohen, G. B., Ren, R., and Baltimore, D. (1995) *Cell* **80**, 237–248
42. Dong, F., Feldmesser, M., Casadevall, A., and Rubin, C. S. (1998) *J. Biol. Chem.* **273**, 6533–6541
43. Carr, D. W., Stofko-Hahn, R. E., Fraser, I. D. C., Acott, T. S., Brennan, R. G., and Scott, J. D. (1991) *J. Biol. Chem.* **266**, 14188–14192
44. Rossi, E. A., Li, Z., Feng, H., and Rubin, C. S. (1999) *J. Biol. Chem.* **274**, 27201–27210
45. Hausken, Z. E., Coghlan, V. M., Hastings, C. A., Reimann, E. M., and Scott, J. D. (1994) *J. Biol. Chem.* **269**, 24245–24251
46. Hausken, Z. E., Dell'Acqua, M. L., Coghlan, V. M., and Scott, J. D. (1996) *J. Biol. Chem.* **271**, 29016–29022
47. Newlon, M. G., Roy, M., Hausken, Z. E., Scott, J. D., and Jennings, P. A. (1997) *J. Biol. Chem.* **272**, 23637–23644
48. Luo, Z., Shafit-Zagardo, B., and Erlichman, J. (1990) *J. Biol. Chem.* **265**, 21804–21810
49. Scott, J. D., Stofko, R. E., McDonald, J. R., Comer, J. D., Vitalis, E. A., and Mangili, J. A. (1990) *J. Biol. Chem.* **265**, 21561–21566
50. Carr, D. W., Stofko-Hahn, R. E., Fraser, I. D., Cone, R. D., and Scott, J. D. (1992) *J. Biol. Chem.* **267**, 16816–16923
51. McLaughlin, S., and Aderem, A. (1995) *Trends Biochem. Sci.* **20**, 272–276
52. Arbuzova, A., Murray, D., and McLaughlin, S. (1998) *Biochim. Biophys. Acta* **1376**, 369–379
53. Swierczynski, S. L., and Blackshear, P. J. (1996) *J. Biol. Chem.* **271**, 23424–23430
54. Seykora, J. T., Myat, M. M., Allen, L. A., Ravetch, J. V., and Aderem, A. (1996) *J. Biol. Chem.* **271**, 18797–18802
55. Swierczynski, S. L., and Blackshear, P. J. (1995) *J. Biol. Chem.* **270**, 13436–13445
56. Arbuzova, A., Wang, J., Murray, D., Jacob, J., Cafiso, D. S., and McLaughlin, S. (1997) *J. Biol. Chem.* **272**, 27167–27177
57. Hartwig, J. H., Thelen, M., Rosen, A., Janmey, P. A., Nairn, A. C., and Aderem, A. (1992) *Nature* **356**, 618–622
58. Myat, M. M., Anderson, S., Allen, L. A., and Aderem, A. (1997) *Curr. Biol.* **7**, 611–614